JOURNAL OF VIROLOGY, Dec. 1993, p. 7461–7471
0022-538X/93/127461-11$02.00/0

Vol. 67, No. 12

Minimum Internal Ribosome Entry Site Required for Poliovirus Infectivity

AURELIA A. HALLER, JOSEPH H. C. NGUYEN, AND BERT L. SEMLER*

Department of Microbiology and Molecular Genetics, College of Medicine, University of California, Irvine, California 92717

Received 12 July 1993/Accepted 20 September 1993

Translation initiation by internal ribosome binding is a recently discovered mechanism of eukaryotic viral and cellular protein synthesis in which ribosome subunits interact with the mRNAs at internal sites in the 5′ untranslated RNA sequences and not with the 5′ methylguanosine cap structure present at the extreme 5′ ends of mRNA molecules. Uncapped poliovirus mRNAs harbor internal ribosome entry sites (IRES) in their long and highly structured 5′ noncoding regions. Such IRES sequences are required for viral protein synthesis. In this study, a novel poliovirus was isolated whose genomic RNA contains two gross deletions removing ~100 nucleotides from the predicted IRES sequences within the 5′ noncoding region. The deletions originated from previously in vivo-selected viral revertants displaying non-temperature-sensitive phenotypes. Each revertant had a different predicted stem-loop structure within the 5′ noncoding region of their genomic RNAs deleted. The mutant poliovirus (Sel-5NC-ΔDG) described in this study contains both stem-loop deletions in a single RNA genome, thereby creating a minimum IRES. Sel-5NC-ΔDG exhibited slow growth and a pinpoint plaque phenotype following infection of HeLa cells, delayed onset of protein synthesis in vivo, and defective initiation during in vitro translation of the mutated poliovirus mRNAs. Interestingly, the peak levels of viral RNA synthesis in cells infected with Sel-5NC-ΔDG occurred at slightly later times in infection than those achieved by wild-type poliovirus, but these mutant virus RNAs accumulated in the host cells during the late phases of virus infection. UV cross-linking assays with the 5′ noncoding regions of wild-type and mutated RNAs were carried out in cytoplasmic extracts from HeLa cells and neuronal cells and in reticulocyte lysates to identify the cellular factors that interact with the putative IRES elements. The cellular proteins that were cross-linked to the minimum IRES may represent factors playing an essential role in internal translation initiation of poliovirus mRNAs.

The genetic information of poliovirus (PV), a member of the *Picornaviridae* family, is encoded in a single-stranded, positive-sense RNA approximately 7,400 nucleotides (nt) in length (24, 47, 51). An unusually long 5′ noncoding region (NCR) (742 nt for PV type 1 [PV1]) precedes the single long open reading frame encoding a giant polypeptide that is cleaved co- and posttranslationally into the structural and nonstructural virus proteins by virus-encoded proteinases (24). A much shorter untranslated region (~65 nt) is present at the 3′ terminus of PV RNA, and this sequence has been implicated to play a role in viral RNA replication (19). The unusual length, the high degree of nucleotide sequence conservation (51), and similar computer-predicted RNA secondary structures of the 5′ NCRs found in the genomic RNAs of the three PV serotypes and other closely related viruses, such as human rhinovirus and coxsackievirus (45), suggest a major role for this RNA segment in the virus life cycle. Indeed, the 5′ NCR of PV RNA has been shown to direct internal ribosome entry (38). Furthermore, it has been suggested that the PV 5′ NCR harbors both the binding site for the viral RNA replicase on the negative-sense RNA and the major determinants responsible for the attenuation or neurovirulence phenotype of PV.

The presence of a genome-linked protein (VPg) at the 5′ end of PV RNA (39) and all other picornavirus genomic RNAs, rather than the 7-methylguanosine cap structure found at the 5′ ends of nearly all eukaryotic mRNAs, precludes the utilization of a cap-dependent mechanism for initiation of protein synthesis. Instead, PVs (42), human rhinoviruses (3), encephalomyocarditis virus (20, 22, 23), foot-and-mouth disease virus (1, 26), and hepatitis A virus (6, 13) have been shown to use cap-independent translation initiation that is directed by RNA sequences and/or RNA structures present in the 5′ NCR forming, collectively, the internal ribosome entry site (IRES). Such a mechanism is not compatible with the scanning mechanism that appears to explain the steps in translation initiation required for ribosome binding to most eukaryotic mRNAs (25, 41).

Members of the family *Picornaviridae* encode two different types of IRES elements that separate the members along phylogenetic lines on the basis of common predicted RNA secondary structures (for reviews, see references 18 and 21). One group contains the enteroviruses and rhinoviruses, and the other group is made up of the aphthoviruses, cardioviruses, and hepatitis A viruses. All picornavirus IRES elements have a polypyrimidine tract that, as has been shown for PV, must be properly spaced from a highly conserved noninitiating AUG codon for maximum efficiency of internal translation initiation (14, 33, 38, 44, 46) (Fig. 1A). The IRES elements of cardio-, entero-, and aphthoviruses interact with the cellular factor p57 found at high levels in rabbit reticulocyte lysate (RRL) (22, 31), a factor now known to be a polypyrimidine tract-binding protein (11, 17, 36). Two other cellular factors, present predominantly in HeLa cells, interact with the IRES element of enteroviruses. One was identified as the La protein (p52) (34, 35), and the other is a 50-kDa factor (8, 37). The roles of these cellular proteins in internal translation initiation for these viruses are not well understood.

For PV, there are seven computer-predicted RNA stem-

* Corresponding author.

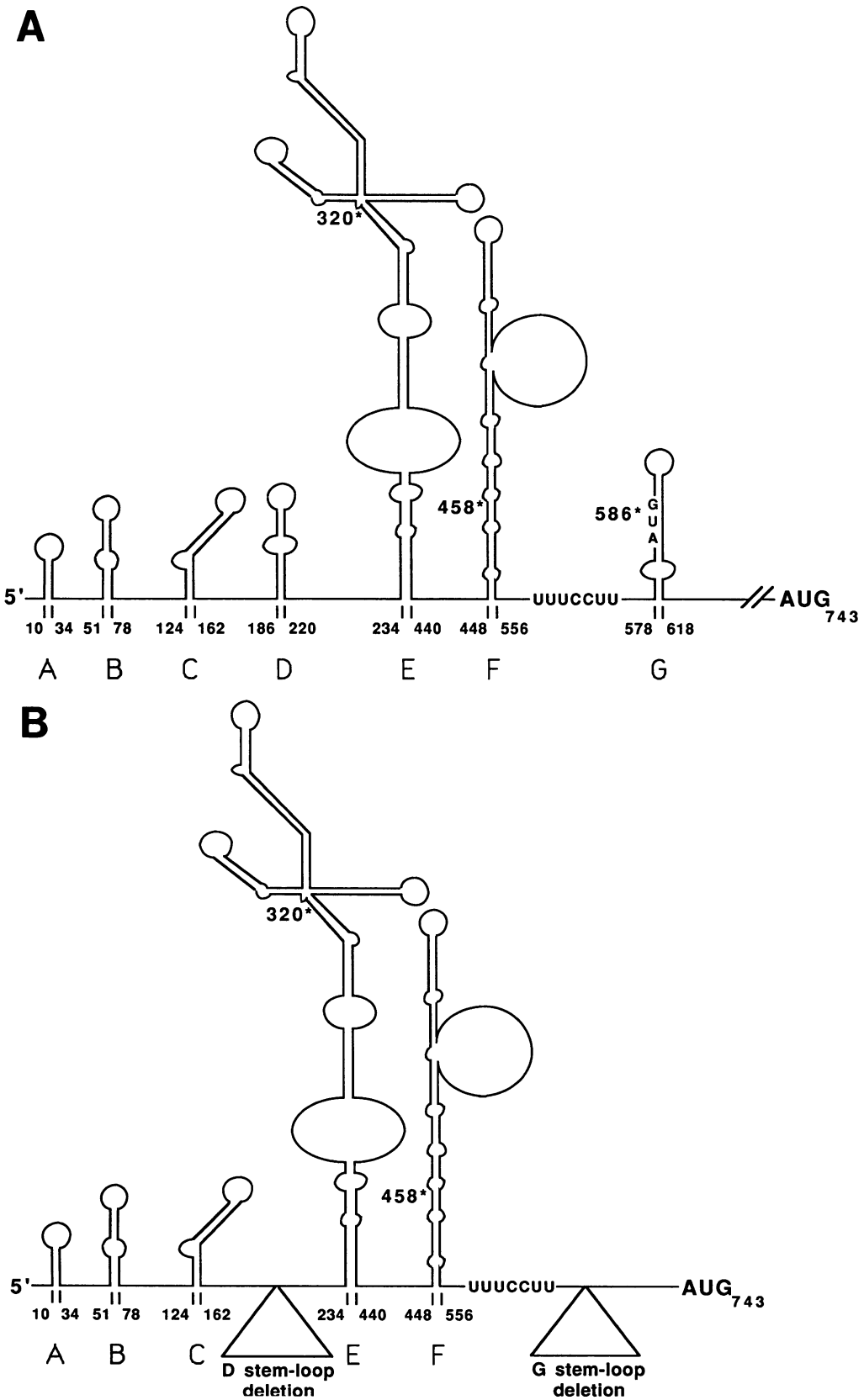

FIG. 1. (A) Diagram of the computer-predicted RNA secondary structures formed by the 5′ NCR of PV RNA. The numbering of nucleotides in the stem-loop structures refers to PV1. The stem-loop structures are labeled A through G. The asterisks denote AUG codons conserved among enteroviruses. UUUCCUU marks the location of the conserved polypyrimidine tract located between stem-loops F and G in PV RNA. The putative IRES element is composed of stem-loops D, E, F, and G. The AUG_{743} represents the authentic translation start codon. (B) Diagram of the 5′ NCR of the ΔDG genome containing the minimum IRES element. Stem-loop structures D and G have been deleted. The polypyrimidine tract is still intact and in close proximity to the translation start codon at position 743.

loops in the 5′ NCR (designated A through G). Stem-loops D, E, F, and G are involved in the formation of the putative IRES element, roughly encompassing 440 nt (from nt 180 to 620) within the 5′ NCR (Fig. 1A) (42, 52). Using precise deletions of single (predicted) stem-loop structures, we previously reported that deletion of stem-loop F is highly detrimental to viral translation initiation and that the altered RNA templates harboring such a deletion are not infectious. In addition, the RNA sequences in stem-loop F must assume their proper conformation to effect normal translation initiation functions (14). It was further shown by RNA electrophoretic mobility shift analysis that RNA templates lacking stem-loop E sequences could not prevent the formation of specific RNA-protein complexes detected for wild-type RNA (containing stem-loop E) (9a). In addition, a recent study employing UV cross-linking assays demonstrated that two cellular proteins of 38 and 48 kDa bind to the PV stem-loop E RNA sequences (12). The above-mentioned 50-kDa cellular protein contacts stem-loop D of the PV 5′ NCR (8, 37), p52 binds to stem-loop G of the 5′ NCR RNA (34), and p57 has been shown to interact with PV sequences between nt 220 and 560 (stem-loops E and F) (44). For the PV1 5′ NCR, the distance between the polypyrimidine tract and a highly conserved, noninitiator AUG codon is ~20 nt. This nucleotide sequence and/or spacing requirement has not been shown to exist for HeLa cell mRNAs (32) or *Drosophila melanogaster* mRNAs (40) capable of directing internal ribosome entry. A comparison of the RNA secondary structure between cellular and viral IRES elements reveals no common sequence or structural features. Thus, it appears difficult, apart from their function, to precisely define IRES elements.

In this study, a novel PV RNA template (ΔDG), harboring a minimum IRES element, was genetically engineered. Two predicted RNA stem-loop structures (D and G) and a major portion of the highly variable region between stem-loop G and the initiator AUG codon at nt 743 within the 5′ NCR were deleted, generating a 5′ NCR containing only 546 nt. Previously in vivo-selected viral revertants containing either the D stem-loop (R2) (9) or G stem-loop deletion (Se1-5NC-PV1X585Δ1) (14) displayed minor or no translation initiation defects, respectively. Interestingly, when these two deletions were combined in the same RNA template (ΔDG), removing ~200 nt from the 5′ NCR, ribosomes still initiated protein synthesis (although at greatly decreased levels) and infectious virus particles were produced following transfection of the mutated RNAs into HeLa cells. The mutant virus displayed a slow growth phenotype and produced pinpoint plaques. An RNA synthesis kinetic analysis revealed not only a delayed onset of RNA synthesis but also an accumulation of virion RNA in infected cells during late phases of the infectious cycle when the wild-type virus had already lysed the host cells. The RNA-protein interactions of the minimum IRES element of the ΔDG RNA were analyzed by UV cross-linking assays to define the factors absolutely essential for internal translation initiation.

MATERIALS AND METHODS

Construction of the ΔDG PV cDNA. The full-length PV cDNA plasmids pT7-PV1X585R1 (14) and R2 (9), present in a pGEM1-pBR322 vector background, containing the G or D stem-loop deletion in the 5′ NCR, respectively, provided the starting material for the genetic manipulations. The R2 mutation was cloned into a previously described plasmid vector, pT7-PV1 (14). A ~5.3-kb *Bgl*I fragment from nt 35 to 5318 derived from the R2 cDNA-containing PV1 sequences, a 1.1-kb *Bgl*I fragment from PV nt 35 to the *Bgl*I site present in the Amp^r gene of pGEM1, and a ~3.5-kb *Bgl*I segment from PV nt 5318 to the *Bgl*I site located in the Amp^r gene (both fragments were derived from pT7-PV1 [14], and both contain PV1 and pGEM1 sequences) were ligated and used to transform *Escherichia coli*. The resulting plasmid was called pT7-R2. The ΔDG PV cDNA plasmid was constructed by ligation of a ~1.1-kb *Bsm*I fragment from PV nt 456 to 1513 derived from pT7-PV1X585R1 (containing the G stem-loop deletion) and an ~8.5-kb *Bsm*I segment from PV nt 456 to 1513 derived from pT7-R2 (containing the D stem-loop deletion and both PV and vector sequences). Relevant nucleotide sequences of plasmids containing the altered cDNAs corresponding to the 5′ NCR were confirmed by DNA sequence analysis.

In vitro transcription of subgenomic and full-length PV cDNA. Subgenomic PV cDNAs were linearized by digestion with restriction endonuclease *Sna*BI (nt 2954) within the P1 coding region. In vitro transcriptions were carried out with bacteriophage T7 RNA polymerase (Pharmacia) as described elsewhere (29), except that RNAs were treated with RNase-free DNase and ethanol precipitated twice to ensure removal of the DNA template and all unincorporated nucleotides. Prior to transcription, full-length PV cDNA plasmids were linearized with restriction endonuclease *Eco*RI. The linearized full-length PV cDNAs were transcribed with T7 RNA polymerase (54), and the synthetic RNAs were used to transfect HeLa cell monolayers without purification.

Transfection of RNAs derived from full-length PV cDNAs. Subconfluent HeLa cell monolayers on 60-mm-diameter plates were transfected with RNA (1 to 5 μg) transcribed from full-length mutant PV cDNAs by the DEAE-dextran-mediated RNA transfection technique modified from the method of Vaheri and Pagano (53). HeLa cell monolayers were rinsed with 2 ml of TS buffer (137 mM NaCl, 4.4 mM KCl, 0.7 mM Na_2HPO_4, 25 mM Trizma base, 5 mM $MgCl_2$, 0.3 μM $CaCl_2$), treated with 0.25 ml of 1 mg of DEAE-dextran per ml and RNA in TS buffer, incubated at room temperature for 30 min, and overlaid with either Dulbecco modified Eagle medium containing 10% fetal calf serum or a semisolid medium consisting of Dulbecco modified Eagle medium, 6% fetal calf serum, and 0.45% agarose. The transfected monolayers were incubated at 33 and 37°C until cytopathic effects or plaques were visible.

Virus stock preparation and plaque assay. The mutant virus stock was prepared by picking well-isolated plaques 3 days after transfection. The plaques were clonally purified by a second round of infection and plaque isolation. The plaque-purified stock was expanded by two serial passages through HeLa cell monolayers. After five freeze-thaw cycles of the mutant P2 virus stocks, the titer was determined on 60-mm-diameter plates of HeLa cell monolayers under semisolid medium at 33 or 37°C.

Sequencing of mutant viral RNA. Viral RNA was prepared by Nonidet P-40 lysis as described by Campos and Villarreal (7). The viral RNA was sequenced by extension of 20-nt synthetic primers corresponding to the complementary strand of nt 633 to 652 (L164) or to nt 272 to 291 (DB5) of PV RNA with [α-^{32}P]dATP, a mixture of deoxynucleotides and dideoxynucleotides, and reverse transcriptase (15, 48).

One-step growth curves. The kinetics of mutant and wild-type viral growth were measured as described previously (2), with some modifications. Briefly, suspension cultures of HeLa cells were infected with PV1 or mutant PV at a multiplicity of infection (MOI) of 10 for 30 min at room temperature. The cells were then rinsed three times with isotonic phosphate-buffered saline (PBS), and the infected cultures were incu-

bated at 33 or 39°C. Supernatant and cells were harvested together at 1, 2, 3, 4, and 6 h at 39°C or at 2, 4, 6, 8, and 10 h at 33°C. The number of PFU per cell present at each time point was determined by plaque assay.

In vitro translation of RNAs. Subgenomic RNAs were translated in the presence of [^{35}S]methionine at 30°C in a RRL (Promega) supplemented with ~15 to 20% (vol/vol) of a HeLa cell or NGP cell (a human neuroblastoma cell line) cytoplasmic extract (49). The RNA concentration in the translation reaction mixtures was 6 μg/ml. Translation reactions were terminated after 3 h by incubation at 30°C with RNase A (200 μg/ml) for 20 min. All reaction mixtures were diluted 10-fold in Laemmli sample buffer and analyzed by sodium dodecyl sulfate (SDS)–10% polyacrylamide gel electrophoresis (29). Autoradiograms of the gels were scanned with an LKB Ultrascan 2 laser densitometer.

Labeling of infected cells with [^{35}S]methionine. Confluent HeLa cell monolayers on 60-mm-diameter plates were infected with the wild-type or mutant virus at a MOI of 10. The virus was allowed to adsorb for 30 min at room temperature, and then the cells were overlaid with 3 ml of methionine-free minimal essential medium containing 10% fetal calf serum and incubated at 37°C. After 2, 4, and 6 h postinfection, 60 μCi of [^{35}S]methionine was added to each plate of infected cells, and the cells were incubated for 2 h at 37°C. The monolayers were then rinsed with PBS, harvested from the plates, pelleted, and resuspended in Laemmli sample buffer (27). After the mixture was boiled, the protein products were fractionated on a SDS–12.5% polyacrylamide gel.

RNA extraction and slot blot analysis. As described previously (9), confluent HeLa cell monolayers were infected with wild-type or mutant virus at a MOI of 10 and incubated at 33, 37, and 39°C. At various times after infection (3, 6, 9, and 12 h), total cytoplasmic RNA was extracted (as described above). A portion of the cytoplasmic RNA (3 μg) was diluted in 10× SSC (1× SSC is 0.15 M NaCl plus 0.015 M sodium citrate) and immobilized on a nitrocellulose membrane with a vacuum slot blot apparatus. Nitrocellulose filters were baked at 80°C for 2 h. Filters were prehybridized for 4 h at 50°C in 5× Denhardt's solution (0.1% polyvinylpyrrolidone, 0.1% Ficoll, 0.1% bovine serum albumin)–6× NET (0.15 M NaCl, 0.1 mM EDTA, 20 mM Tris-HCl, pH 8.0)–0.1% SDS. PV-specific deoxynucleotides were labeled with [γ-^{32}P]ATP, using T4 polynucleotide kinase, and then purified from unincorporated isotope over a G-50 Sephadex column. The radiolabeled oligonucleotides were added after the prehybridization step at a concentration of 10^6 cpm/ml and hybridized at 50°C for 24 h. Filters were washed four times in 6× NET–0.5% SDS for 10 min at room temperature and once at 50°C for 5 min. Hybridized filters were exposed to XAR film and quantitated by laser densitometric scanning.

Preparation of cellular extracts. The preparation of the S10 cytoplasmic extracts from HeLa cells and the ribosomal salt wash preparation have been described previously (5, 16). The neuronal extract from suspension NGP cells was prepared in essentially the same manner. NGP cells are semiadherent, human neuroblastoma cells that we have adapted for growth in suspension cultures (4, 49). The suspension cultures of NGP cells are grown in minimal essential medium supplemented with 10% fetal calf serum and 10% bovine serum.

UV cross-linking of cellular proteins to PV RNA. UV cross-linking assays were performed as described previously with some modifications (22). The [^{32}P]UTP-labeled, high specific activity transcripts from nt 1 to 815 (1.5×10^7 cpm/μg) were generated by in vitro transcription from the full-length mutated and wild-type cDNAs linearized with the restriction endonuclease *Ase*I. The RNAs were quantitated by liquid scintillation counting of aliquots that had been spotted on DE81 filters and treated extensively with dibasic sodium phosphate to remove unincorporated nucleotides. The labeled RNAs were also subjected to electrophoresis on denaturing polyacrylamide gels to ensure that the RNAs were intact. An aliquot of RNA containing 6×10^6 cpm (1.5 pmol) was used for each cross-linking reaction. Extracts from HeLa or NGP cells (100 μg) or RRL (280 μg) were incubated with 20 μg of poly(rI-rC) in binding buffer (25 mM KCl, 5 mM HEPES [*N*-2-hydroxyethylpiperazine-*N*′-2-ethanesulfonic acid] [pH 7.8], 10 mM $MgCl_2$, 0.1 mM EDTA, 150 mM NaCl, and 3.8% glycerol [final concentrations]) at 30°C for 15 min in a total reaction volume of 19 μl. The radiolabeled synthetic RNAs were then added, and the reactions were incubated for 15 min at 30°C. After irradiation in a UV Stratalinker 1800 (Stratagene) at 254 nm for 10 min on ice, an RNase cocktail (30 μg of RNase A, 30 μg of RNase T_1, 0.3 U of RNase T_2, and 0.1 U of RNase V_1) was added to the reaction mixtures, and the mixtures were incubated at 37°C for 30 min. Finally, an equal volume of 2× Laemmli sample buffer was added. After the mixture was boiled, the samples were analyzed on a SDS–12.5% polyacrylamide gel.

RESULTS

Characterization of the mutant ΔDG virus. In previous studies carried out by Dildine and Semler (9) and Haller and Semler (14), two viral revertants were isolated in which each had a different predicted stem-loop structure of the 5′ NCR of PV RNA deleted. The R2 viral revertant had a 45-nt deletion corresponding to the complete stem-loop D (from nt 184 to 228), displayed a small plaque phenotype, and had no significant translation initiation defect, although it exhibited a delay in achieving peak levels of RNA synthesis compared with wild-type virus during infection of HeLa cells (9, 10). Se1-5NC-X585Δ1 had the entire stem-loop G removed as well as most of the highly variable region upstream of the initiation AUG at position 743 (from nt 564 to 715), thereby deleting 151 nt of the 5′ NCR. Interestingly, this PV revertant (Se1-5NC-X585Δ1) exhibited an efficiency of translation initiation equivalent to wild-type levels and displayed a small plaque phenotype (14). Both of these mutants displayed non-temperature-sensitive phenotypes similar (but not identical) to those of wild-type virus with regard to viral protein and RNA synthesis. These results suggested that neither stem-loop D or G, implicated to be part of the internal ribosome entry site (52), was absolutely required for virus growth in tissue culture. We were interested in the effect(s) on viral functions if both of these in vivo-selected deletions were present in the same viral RNA template. The two deletions together shorten the 5′ NCR by ~200 nt and thus create a minimum functional IRES element (Fig. 1B). If either stem-loop D or G were redundant for functions that either one supplies during initiation complex formation on PV mRNA, deletion of both structures would result in a nonfunctional RNA template for protein synthesis. To test whether the genetically altered mRNAs would produce infectious virus, the in vitro-synthesized RNAs were transfected into HeLa cells and assayed for virus production at two temperatures (33 and 37°C). Virus plaques were observed 3 days after transfection at both temperatures, suggesting that stem-loops D and G could both be deleted in the same RNA template without abolishing virus infectivity. After two rounds of plaque purification, P1 and P2 virus stocks of mutant Se1-5NC-ΔDG were grown and subsequently characterized. The locations of the deletions in the 5′ NCR of the viral RNA

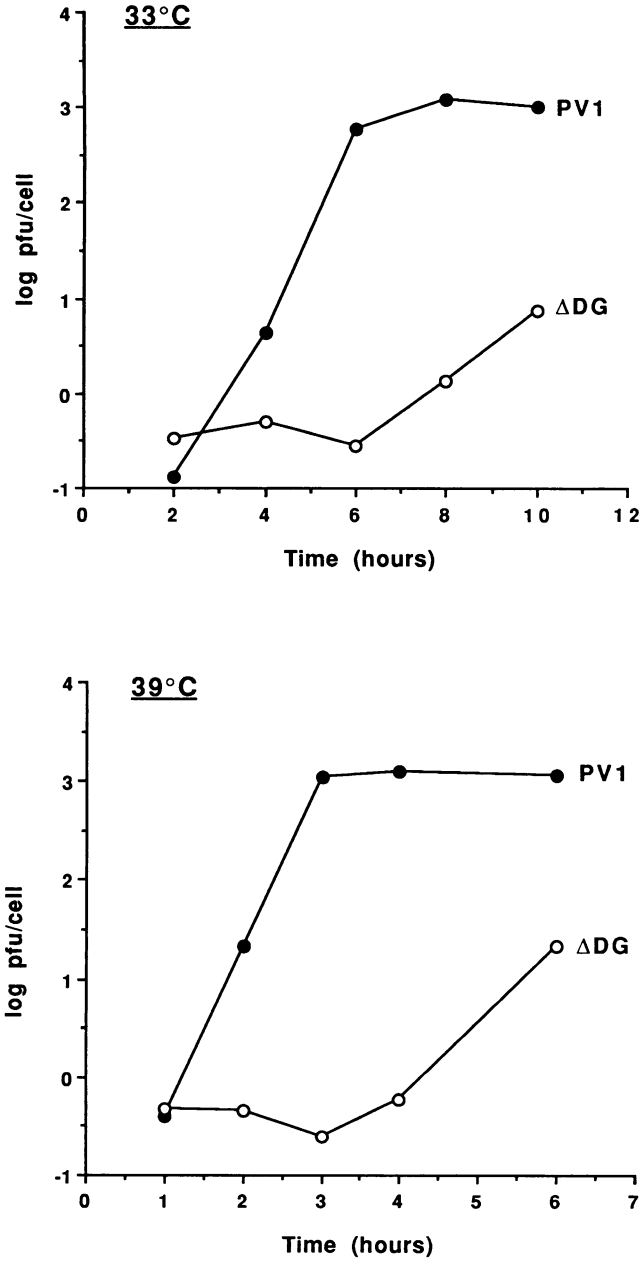

FIG. 2. Kinetics of virus production in HeLa cells infected with Se1-5NC-ΔDG or wild-type PV at 33 and 39°C. Suspension cultures of HeLa cells at a density of 6×10^5 cells per ml were infected with the mutant (ΔDG) or wild-type (PV1) virus and incubated for 30 min at room temperature. The cells were harvested at the time points given, and the numbers of PFU per cell were determined by plaque assay.

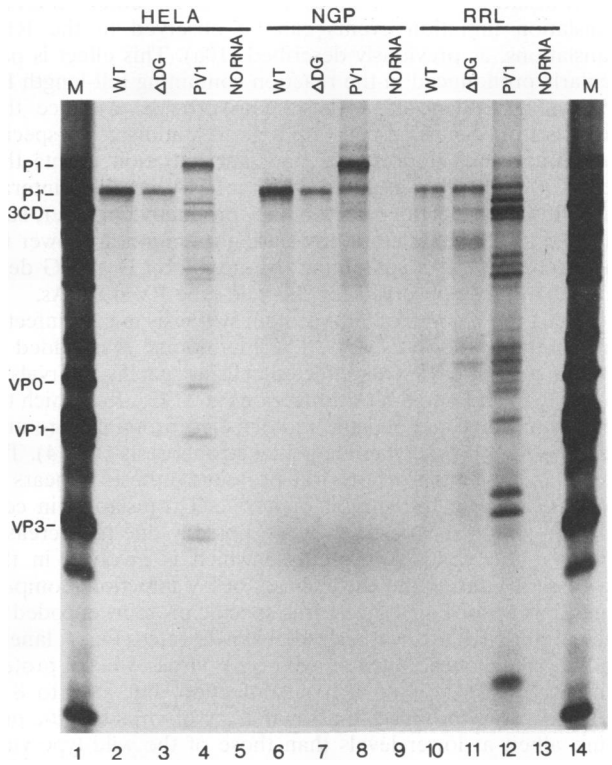

FIG. 3. In vitro translation of subgenomic transcripts from ΔDG and wild-type cDNAs. The cDNA templates were truncated within the P1 region, and transcripts derived from these templates were translated in vitro as described in Materials and Methods. The translation products were resolved on an SDS–10% polyacrylamide gel. Lanes 2 to 5 show the RRL translation reactions supplemented with HeLa S10, lanes 6 to 9 represent RRL translations supplemented with an S10 from NGP cells, and lanes 10 to 13 show RRL translations alone. Lanes: M, marker lane of [^{35}S]methionine-labeled proteins from HeLa cell monolayers infected with wild-type PV; WT, wild-type cDNA; NO RNA, no RNA was added to an in vitro translation reaction; PV1, a positive control using full-length transcripts from the plasmid pT7-PV1 containing a complete cDNA of the wild-type PV1 genome.

were confirmed by RNA sequence analysis. Se1-5NC-ΔDG displayed a pinpoint plaque phenotype when grown on HeLa cells at both 33 and 37°C. A one-step growth analysis of Se1-5NC-ΔDG revealed a reduction of virus growth in HeLa cells of ~2 log units compared with that of wild-type virus at both 33 and 39°C (Fig. 2). However, the mutant virus did not display a temperature-sensitive phenotype for growth at 39°C.

In vitro translation efficiencies and mutant viral protein synthesis. To determine whether the introduced deletions of stem-loops D and G impair translation initiation of PV RNA, mutated and wild-type RNAs truncated in the P1 coding region of the polyprotein were assayed in vitro in a RRL cell-free translation system alone or supplemented with a HeLa cell or neuroblastoma cytoplasmic extract. The translation products were analyzed on an SDS–10% polyacrylamide gel (Fig. 3). Subgenomic mRNAs were used in these translation experiments that result in a single protein product which greatly facilitates the analysis of the translation efficiencies of these templates. In this manner, the P1 region of the PV genome serves as a reporter gene. For quantitation of the translation efficiencies of the mutated RNAs, the autoradiogram was scanned with a laser densitometer. As shown in Fig. 3, the translation initiation efficiency of the ΔDG mRNAs was ~35% of the levels observed for wild-type mRNAs in the reactions supplemented with HeLa S10 (compare lanes 2 and 3). A similar effect was observed when neuronal S10 was added to the translation reactions. The ΔDG mRNA directed translation at levels ~3-fold lower (~30%) than those of the wild-type mRNA of PV (Fig. 3, lanes 6 and 7). In contrast, in translation reactions carried out solely in RRL, both mutated and wild-type mRNAs represent equally inefficient templates

for translation (Fig. 3, lanes 10 and 11). Some aberrant translation initiation events can be observed in the RRL translations, as previously described (10a). This effect is particularly pronounced in the reaction containing full-length PV RNA (Fig. 3, lane 12). These data provide evidence that extracts from neuronal cells are able to stimulate PV-specific translation and suppress the aberrant initiation events that occur in RRL. The mutated ΔDG mRNA may not interact with all of these cellular factors in a productive manner, such that the levels of authentic translation initiation are lower for the altered mRNAs containing the stem-loop D and G deletions than those observed for the wild-type PV mRNAs.

To test the kinetics of viral protein synthesis in cells infected with mutant Se1-5NC-ΔDG, [^{35}S]methionine was added to mutant or wild-type virus-infected cells at specific intervals (2 to 4, 4 to 6, and 6 to 8 h postinfection) at 37°C, after which the cells were harvested and the radiolabeled proteins were analyzed by SDS-polyacrylamide gel electrophoresis (Fig. 4). The defect in the initiation of viral protein synthesis appears to cause a delay in the shutoff of host cell translation in cells infected with Se1-5NC-ΔDG virus, possibly due to decreased levels of the viral 2A proteinase which is involved in this process (30) during the early phases of PV infection (compare lanes 2 and 5 of Fig. 4). All virus-specific proteins encoded by the mutant virus are synthesized at slower rates (Fig. 4, lanes 2 and 5) than those of the wild-type virus, whose protein synthesis peaks at 4 to 6 h postinfection, but at 6 to 8 h, Se1-5NC-ΔDG produces a normal array of virus-specific proteins, albeit at lower levels than those of the wild-type virus (lanes 2, 3, and 6). These results indicate that the deletions of stem-loops D and G in the 5′ NCR RNA affect the initiation step of protein synthesis and not viral protein processing. Interestingly, VP2, a capsid protein generated in virions after the maturation cleavage of precursor protein VP0, can be detected only at very low levels in cells infected by the mutant virus even at 6 to 8 h after infection (Fig. 4, lanes 2 and 6). This observation correlates well with the low number and the small burst size of the infectious virus particles produced by Se1-5NC-ΔDG at 6 h postinfection in the one-step growth experiments (Fig. 2).

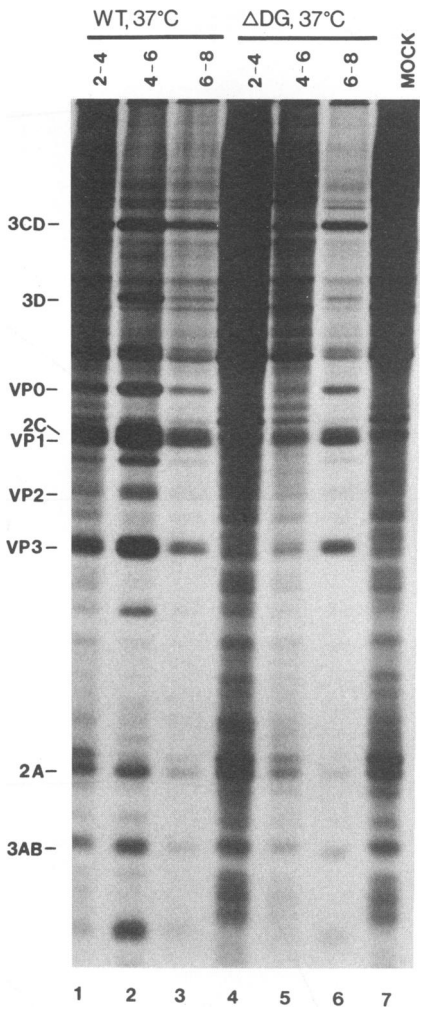

FIG. 4. [^{35}S]methionine labeling of HeLa cells infected with mutant (ΔDG) or wild-type (WT) PV. HeLa cell monolayers were infected at an MOI of 10 and were incubated at 37°C. Infected cells were pulse-labeled with [^{35}S]methionine for the indicated 2 h periods from 2 to 4, 4 to 6, and 6 to 8 h postinfection. Viral proteins are shown on the left of the panel. Lane MOCK, samples derived from mock-infected HeLa cells labeled from 4 to 6 h after mock infection at 37°C. After harvesting, the samples were resuspended in Laemmli sample buffer and subjected to electrophoresis on an SDS–12.5% polyacrylamide gel.

RNA synthesis kinetics of Se1-5NC-ΔDG. Since the gross deletions in the 5′ NCR of Se1-5NC-ΔDG may have perturbed replicase binding signals present at the 3′ ends of minus-strand RNAs, it was of interest to determine whether the deletion of the stem-loop elements D and G in the 5′ NCR of PV RNA had an effect on viral RNA synthesis, in addition to the observed effects on translation initiation. As the growth of mutant Se1-5NC-ΔDG was sensitive to actinomycin D (14a), RNA synthesis kinetics for this virus could not be determined by measuring [^{3}H]uridine incorporation into the viral RNA in infected cells. Instead, 60-mm-diameter plates of confluent HeLa cells were infected with either the mutant or wild-type virus and incubated at 33, 37, or 39°C. The virus-infected cells were harvested at 3, 6, 9, and 12 h postinfection, and total cytoplasmic RNA was isolated. The cytoplasmic RNA was blotted onto nitrocellulose and probed with radiolabeled PV-specific deoxyoligonucleotide (Fig. 5A). At 9 h postinfection, when wild-type RNA synthesis peaked at 33°C, the RNA produced by the mutant virus at 33°C was barely detected (Fig. 5B). Thus, RNA synthesis of Se1-5NC-ΔDG was delayed at 33°C, perhaps because of the translation initiation defect that resulted in a decreased production of viral proteins necessary for RNA replication. At 37°C, the levels of mutant RNA synthesis were similar to those observed for the wild-type virus. Note that at 12 h postinfection, most of the wild-type RNA had been packaged and the virion particles have lysed the host cells. In contrast, very high levels of intracellular ΔDG virion RNA were detected in the cells infected with Se1-5NC-ΔDG (Fig. 5A and C). The same effect was observed at 39°C (compare the 6- and 9-h time points in Fig. 5A and D), resulting in a high-level accumulation of mutant virus RNA genomes in the host cells during the late phases of Se1-5NC-ΔDG infection. Apparently, the mutant virion RNAs are not packaged efficiently into the virus capsids, and thus, the progeny virus RNAs accumulate in the host cell. These data imply either that the putative viral RNA packaging signals were deleted in the ΔDG RNA or that the virus capsid proteins were not produced in sufficient quantities in the cells infected with Se1-5NC-ΔDG.

RNA-protein interactions of the 5′ NCR of the mutated viral mRNA. Since the RNA template containing gross deletions of stem-loops D and G in the 5′ NCR was infectious, some of the

RNA-protein interactions observed for this minimum IRES element must be essential for internal translation initiation. UV cross-linking studies were carried out with ^{32}P-labeled wild-type and mutated RNA templates containing PV sequences from nt 1 to 815 (Fig. 6). For comparison to our data obtained from in vitro translations, we tested three different types of cellular extracts in these binding studies, a ribosomal salt wash fraction from either HeLa cells or neuroblastoma cells (NGP), and RRL. It should be noted that the binding pattern we observed with the ribosomal salt wash fractions is the same as that seen with cellular S10 extracts. The observed cross-linked proteins were numbered contiguously from 1 to 13 (Fig. 6). As expected, some of the RNA-protein interactions observed for the wild-type RNA were lost when the mutated template was used. Other factors appeared to bind with a greatly reduced affinity to the ΔDG RNA (Fig. 6). In binding studies with HeLa cellular extracts, a 52-kDa protein (protein 5) and a 48-kDa protein (protein 7) cross-linked to the wild-type RNA but not to the ΔDG RNA (Fig. 6, lanes 1 and 2). Note that the cross-linking of the 50-kDa factor (protein 6) appears to be the result of a nonspecific RNA-protein interaction (14a). A 52-kDa protein that is abundant in HeLa cells was shown previously to interact with stem-loop G sequences (nt 559 to 624) of PV RNA (34). This protein would not be expected to interact with the mutated RNA template, since its binding site was deleted. As shown in Fig. 6, the ~52-kDa protein (protein 5) is absent in the lanes containing the mutant ΔDG RNA as a template. A 50-kDa HeLa cell protein was reported to bind to stem-loop D of the PV 5′ NCR (8, 37). This protein would also not be expected to bind to the ΔDG RNA, since its stem-loop D binding site was deleted. A ~48-kDa protein (protein 7) present in HeLa cells was not detectable in UV cross-linking studies with the ΔDG RNA (Fig. 6, lanes 1 and 2). The molecular mass of this protein in our assay system appears to be closer to ~48 kDa, perhaps as a result of slightly different polyacrylamide gel electrophoresis conditions. Thus, this ~48-kDa protein may indeed represent the 50-kDa protein that binds to stem-loop D. The 42- (protein 8) and 36-kDa (protein 10) cellular proteins in a HeLa cell cytoplasmic extract display a dramatic reduction in binding to the minimum IRES of the ΔDG RNA compared with their interaction with the wild-type 5′ NCR. The 32- (protein 11) and 39-kDa (protein 9) cellular factors do not appear to interact with the 5′ NCR of the mutated RNA.

The proteins present in neuronal extracts display a RNA binding pattern that is very similar to that of extracts derived from HeLa cells (Fig. 6, lanes 3 and 4). Interestingly, the p39 factor (protein 9) appears to be abundant in the extracts from neuroblastoma cells or it exhibits a strong binding affinity for the wild-type PV IRES element. A novel neuronal protein (~60-kDa; protein 12) appears to interact with both the mutated and wild-type 5′ NCRs, and the 68-kDa factor (protein 4) present in HeLa cells is apparently absent in NGP cells.

The UV cross-linking studies using RRL showed that four factors (p39, p48, p52, and p64) interact with the 5′ NCR of the wild-type RNA (Fig. 6, lane 5). As expected from results discussed above, neither p39 (protein 9), p48 (protein 7), or p52 (protein 5) appears to bind to the 5′ NCR RNA of the ΔDG template (Fig. 6, lane 6), while the 64-kDa factor (protein 13) interacts with both wild-type and ΔDG RNA templates. The molecular masses of the majority of the proteins in RRL that bind to the PV 5′ NCR are similar to those of proteins detected in binding reactions with HeLa or NGP extracts. Thus, they may represent related proteins in the

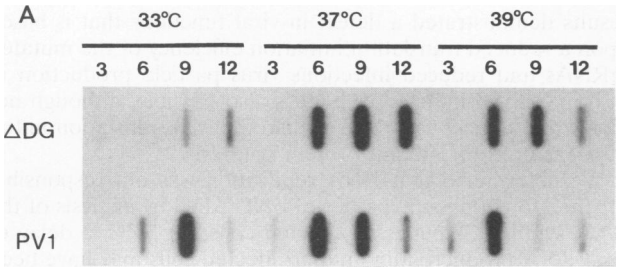

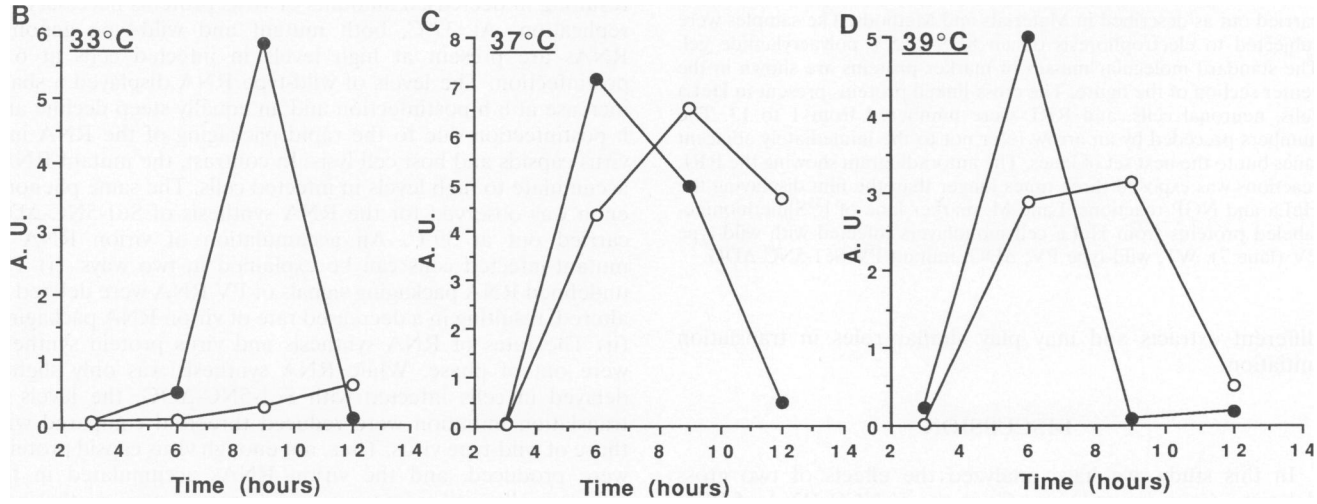

FIG. 5. (A) RNA synthesis of HeLa cells infected with Se1-5NC-ΔDG (ΔDG) or wild-type PV (PV1). HeLa cell monolayers were infected at an MOI of 10 and incubated at 33, 37, or 39°C. At the indicated times (hours) postinfection, total cytoplasmic RNA was prepared from the infected cells as described in Materials and Methods. Samples (3 μg) of RNA were immobilized on nitrocellulose filters with a vacuum slot blot apparatus. The blot was hybridized to ^{32}P-labeled deoxyoligonucleotide probes specific for the PV genome. The autoradiograph was quantitated by laser densitometric scanning. (B to D) Graphs of RNA synthesis of the wild-type and mutant PV as quantitated by laser densitometric scanning of the various time points at 33, 37, and 39°C. A.U. refers to arbitrary units assigned to the values obtained from the densitometric scanning of the autoradiograph. Symbols: ●, wild-type virus; ○, Se1-5NC-ΔDG virus.

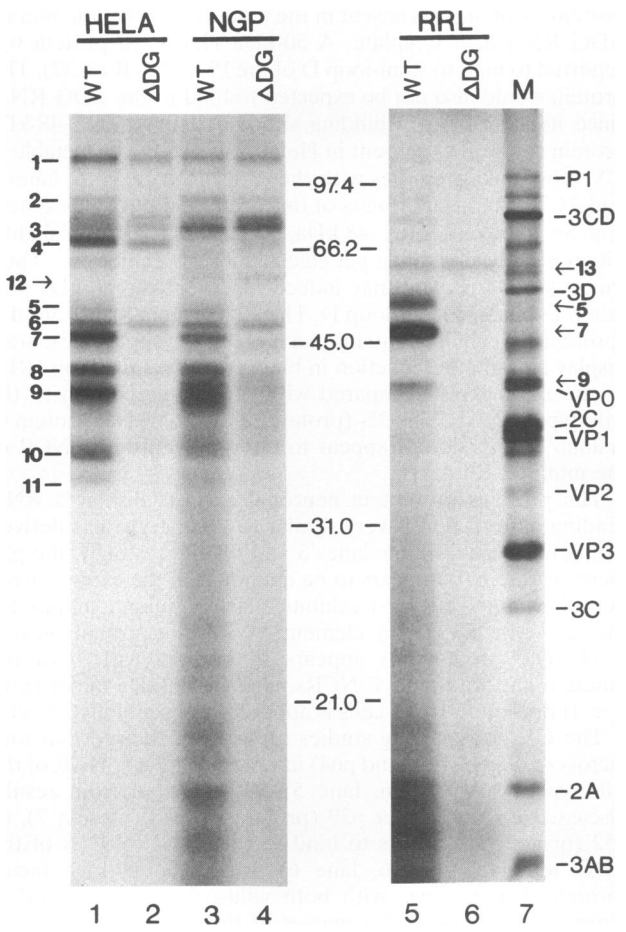

FIG. 6. UV-induced cross-linking of proteins present in HeLa cells, neuronal cells (NGP), and rabbit reticulocyte lysate (RRL) to the 5′ NCR RNAs (from nt 1 to 815) of wild-type and mutant PV. Lanes 1 and 2 show cross-linking in HeLa cell extracts, lanes 3 and 4 are reactions with neuronal extracts, and lanes 5 and 6 show cross-linking reactions carried out with RRL. The UV cross-linking reactions were carried out as described in Materials and Methods. The samples were subjected to electrophoresis on an SDS–12.5% polyacrylamide gel. The standard molecular masses of marker proteins are shown in the center section of the figure. The cross-linked proteins present in HeLa cells, neuronal cells, and RRL were numbered from 1 to 13. The numbers preceded by an arrow refer not to the immediately adjacent lanes but to the next set of lanes. The autoradiogram showing the RRL reactions was exposed three times longer than the film displaying the HeLa and NGP reactions. Lane M, marker lane of [^{35}S]methionine-labeled proteins from HeLa cell monolayers infected with wild-type PV (lane 7). WT, wild-type PV; ΔDG, mutant PV Se1-5NC-ΔDG.

different extracts and may play similar roles in translation initiation.

DISCUSSION

In this study, we have analyzed the effects of two gross deletions (stem-loops D and G) in the 5′ NCR RNA of PV1, removing approximately 200 nt from the 5′ NCR, on internal translation initiation and virus infectivity. The nucleotide deletions originated from two separate virus isolates previously described (9, 14). These pseudorevertants had non-temperature-sensitive growth phenotypes and were similar (but not identical) to wild-type virus. To further define the minimal RNA sequences required for a functional IRES element and to investigate the possibility of RNA stem-loop cross-talk, both deletions were introduced into the same PV RNA genome. Surprisingly, the mutated RNA template (ΔDG) was infectious upon RNA transfections into HeLa cells, although the resulting virus produced yields that were 2 log units lower than those of wild-type virus at both 33 and 39°C. The Se1-5NC-ΔDG virus was not temperature sensitive for growth in HeLa cells at 39°C but displayed a pinpoint plaque phenotype.

In an attempt to analyze the molecular nature of the defect that this virus contained, in vitro translations with wild-type and mutated RNAs, both linearized within the P1 coding region, were carried out. The ΔDG RNAs directed levels of in vitro protein synthesis that were ~30% of the levels observed for wild-type mRNAs. Similar results were observed for in vitro translations that contained neuroblastoma cytoplasmic extract, while the translations that were carried out in RRL showed only basal levels of P1 protein produced for both wild-type and mutated RNAs. These data suggest that a decrease in virus-specific translation initiation occurs at the authentic AUG codon for the mutated ΔDG RNAs. This notion was further supported by [^{35}S]methionine labeling of viral proteins produced by PV-infected cells. As displayed in Fig. 4, even at 6 to 8 h postinfection, the levels of all virus proteins were reduced in cells infected with Se1-5NC-ΔDG. The translation defect also had an effect on the shutoff of host cell protein synthesis (see 4- to 6-h time point), most likely as a result of decreased levels of the virus-encoded 2A proteinase which indirectly activates this event (30). Collectively, our results demonstrated a defect in viral functions that is based upon a reduced translation initiation efficiency of the mutated mRNAs and reduced infectious virus particle production in Se1-5NC-ΔDG-infected cells. It is also possible, although not likely, that a mechanism other than internal translation initiation was used for mutant protein synthesis.

We determined that RNA replication was not responsible for the growth phenotype of Se1-5NC-ΔDG by analysis of the RNA synthesis kinetics in infected cells. At 33°C, a delay of viral RNA production in mutant-infected cells may have been a consequence of the slow onset of viral protein synthesis, resulting in decreased amounts of virus proteins necessary for replication. At 37°C, both mutant and wild-type genomic RNAs are present at high levels in infected cells at 6 h postinfection. The levels of wild-type RNA displayed a sharp increase at 6 h postinfection and an equally steep decline at 9 h postinfection due to the rapid packaging of the RNA into virus capsids and host cell lysis. In contrast, the mutant RNAs accumulate to high levels in infected cells. The same phenomenon was observed for the RNA synthesis of Se1-5NC-ΔDG carried out at 39°C. An accumulation of virion RNA in mutant-infected cells can be explained in two ways. (i) The undefined RNA packaging signals of PV RNA were deleted or altered, resulting in a decreased rate of virion RNA packaging. (ii) The rates of RNA synthesis and virus protein synthesis were out of phase. While RNA synthesis was only slightly delayed in cells infected with Se1-5NC-ΔDG, the levels of translation initiation were reduced threefold compared with those of wild-type virus. Thus, not enough virus capsid proteins were produced, and the virion RNAs accumulated in the infected cells until more virus capsid proteins were synthesized. These results confirm that virus proteins involved in RNA synthesis are required at vastly lower levels than those of the structural proteins.

The limited production of viral proteins in cells infected with mutant Se1-5NC-ΔDG appeared to affect virus assembly and RNA replication differentially. In preliminary experiments, we

attempted to supply additional amounts of virus capsid proteins to Sel-5NC-ΔDG-infected cells to enhance viral RNA packaging and host cell lysis. RNAs (containing the PV 5′ NCR) that encoded the P1 capsid precursor under the control of a T7 phage promoter were transfected with lipofectin into HeLa cells together with vaccinia virus expressing the bacteriophage T7 RNA polymerase (50). Four hours later, the transfected cells were superinfected with Sel-5NC-ΔDG. At various times after infection, the cells were harvested and assayed for infectious virus production by plaque assay (data not shown). Our results did not reveal an increase in the number of PFU per cell in the presence of additional RNAs encoding capsid precursor polypeptides. However, the size of the mutant plaques increased markedly (14a). This size increase may have been due to an increase in burst size of Sel-5NC-ΔDG and implies that a greater number of infectious virus particles was produced from each infectious center. Thus, the RNAs from the mutant virus may have been packaged more efficiently in the presence of higher levels of capsid proteins.

Since the minimum IRES element of Sel-5NC-ΔDG still contained a functional RNA template for internal translation initiation, the cellular proteins interacting with this RNA segment may, in part, mediate the internal ribosome entry process. RNA UV cross-linking assays were carried out in the presence of HeLa or NGP cytoplasmic extracts or RRL with the radiolabeled wild-type or mutated RNAs. Interestingly, various interactions observed for the wild-type RNA template were lost or greatly reduced with the ΔDG RNA template. Our data showed that two proteins with molecular masses of ~48 and 52 kDa bind to the wild-type 5′ NCR of PV RNA. However, these interactions were lost with the ΔDG RNA. These two proteins may represent the previously identified cellular factors, p50 and p52, reported to interact with stem-loops D and G, respectively (8, 34, 37), since their binding sites were removed in the ΔDG mutated RNA. Our results suggest that the RNA-protein interactions involving p50 or p52 are not absolutely required for internal ribosome entry. However, these macromolecular interactions may be essential for obtaining an important stimulatory effect of internal translation initiation.

The proteins present in HeLa cytoplasmic extracts that interact with the minimum IRES of ΔDG RNA have approximate molecular masses of >100, 90, 70, 68, 42, and 36 kDa. The cross-linking efficiencies of the latter two proteins were dramatically reduced with the ΔDG RNA. Gebhard and Ehrenfeld reported the specific interaction of three HeLa cell proteins of similar molecular masses with the PV 5′ NCR RNA, 54-, 48-, and 38-kDa factors (12). However, specific identification requires the isolation of these factors and the generation of specific antibodies directed at these proteins.

Our cross-linking studies with wild-type and ΔDG RNAs in the presence of extracts derived from neuronal cells revealed a similar pattern to that observed in assays using HeLa cell extracts, with two notable exceptions. Cross-linking of a 68-kDa protein was not detected in extracts from neuronal cells, and a novel 60-kDa factor was present in these same extracts that interacts equally well with the wild-type and ΔDG RNAs. LaMonica et al. have previously shown that the attenuation phenotype of PV is correlated with a reduced translation initiation efficiency of PVs in neuronal cells (28). This effect may be the result of a specific interaction with proteins present only in neuronal cells or the lack of a necessary factor (present in HeLa cells), producing reduced levels of protein synthesis in these cells. Therefore, the 60- and 68-kDa proteins may be involved not only in internal translation initiation but also in determination of the attenuation phenotype of PV.

It has been previously reported that in vitro translation of PV mRNAs in RRL results in the production of spurious translation products that are the result of aberrant initiation at internal sites within the coding region of viral RNA (10a). Nevertheless, it was of interest to identify factors present in RRL which interact with the PV IRES element, since these interactions may be involved in selected steps of initiation of virus protein synthesis. Four major proteins with molecular masses of 39, 48, 52, and 64 kDa were cross-linked to the 5′ NCR of wild-type RNA. Surprisingly, only the 64-kDa factor could be cross-linked to the RNA containing the ΔDG 5′ NCR. These data suggest a role for the 64-kDa factor in translation initiation for PV mRNA.

Recently, Hellen et al. reported that a 57-kDa protein (p57) which specifically binds to the 5′ NCR of encephalomyocarditis virus RNA is identical to the nuclear polypyrimidine tract-binding protein (17). In in vitro translation experiments, it was shown that antibodies to polypyrimidine tract-binding protein could prevent translation of encephalomyocarditis virus and PV RNAs. However, translation of encephalomyocarditis virus and PV mRNAs in a HeLa cell cytoplasmic extract that had been immunodepleted with anti-polypyrimidine tract-binding protein serum could not be restored upon addition of purified pyrimidine tract-binding protein. These data suggest that p57 may interact closely with another cellular factor(s) that is also removed in the immunodepleted extract, in agreement with our results showing the absence of cross-linking of a 57-kDa protein to the 5′ NCR of PV RNA (Fig. 6). The p57-associated cellular protein(s) may play an essential role in internal ribosome entry of PV mRNAs, while the presence of p57 could augment the levels of internal translation initiation.

The results described in this study, when coupled with previous data which defined the upper limits of the IRES sequences in the PV 5′ NCR (42, 52), suggest that stem-loop E, stem-loop F, and the polypyrimidine tract may be the only sequence elements that are absolutely required for baseline translation initiation mediated by an internal ribosome entry mechanism. Percy et al. have implicated the involvement of stem-loop C of the 5′ NCR RNA in PV translation initiation (43). These latter conclusions originate from studies that employed bicistronic cDNA constructs linked to two reporter genes to determine the translation efficiencies of various mutated 5′ NCRs transfected into cultured cells in the presence or absence of full-length PV cDNAs. Interestingly, a construct containing a stem-loop C deletion resulted in a loss of the reporter gene product from the second cistron. However, further experimental evidence may be required to show unequivocally that stem-loop C is part of the IRES. For example, a PV mRNA containing a stem-loop C deletion could be transfected into cells to determine whether infectious virus is recovered. Also, the efficiency of in vitro translation initiation directed by such an RNA could be analyzed in a cell-free translation system.

Our study shows that neither stem-loop D or G of the 5′ NCR of PV RNA represent absolutely essential structural components for internal ribosome entry. The RNA-protein interactions involving these stem-loop elements and cellular factors, however, appear to be crucial for important stimulatory activities required to achieve maximum levels of internal translation initiation. Results from these experiments, coupled with those obtained from functional assays of RNA-protein interactions in the PV 5′ NCR, will be required to ultimately sort out the events leading to successful translation initiation on the unusual mRNAs produced in picornavirus-infected cells.

ACKNOWLEDGMENTS

We thank Holger Roehl and Jonathan Towner for critical comments on the manuscript. We are grateful to Eric Stanbridge for the generous gift of the neuroblastoma cell line. We also thank Xi-Yu Jia and Donald Summers for advice on the use of lipofectin in uptake assays.

This work was supported by Public Health Service grant AI26765 and by core support from the Irvine Research Unit in Animal Virology (University of California, Irvine, Calif.). A.A.H. is supported by a predoctoral traineeship from the National Institutes of Health (GM 07134-18).

REFERENCES

1. **Belsham, G. J., and J. K. Brangwyn.** 1990. A region of the 5′ noncoding region of foot-and-mouth disease virus RNA directs efficient internal initiation of protein synthesis within cells: involvement with the role of L protease in translational control. J. Virol. **64:**5389–5395.
2. **Blair, W. S., S.-S. Hwang, M. F. Ypma-Wong, and B. L. Semler.** 1990. A mutant poliovirus containing a novel proteolytic cleavage site in VP3 is altered in viral maturation. J. Virol. **64:**1784–1793.
3. **Borman, A., and R. J. Jackson.** 1992. Initiation of translation of human rhinovirus RNA: mapping the internal ribosome entry site. Virology **188:**685–696.
4. **Brodeur, G. M., G. S. Sekhon, and M. N. Goldstein.** 1977. Chromosomal aberrations in human neuroblastomas. Cancer **40:** 2256–2263.
5. **Brown, B. A., and E. Ehrenfeld.** 1979. Translation of poliovirus RNA *in vitro*: changes in cleavage pattern and initiation sites by ribosomal salt wash. Virology **97:**396–405.
6. **Brown, E. A., S. P. Day, R. W. Jansen, and S. M. Lemon.** 1991. The 5′ nontranslated region of hepatitis A virus RNA: secondary structure and elements required for translation in vitro. J. Virol. **65:**5828–5838.
7. **Campos, R., and L. P. Villarreal.** 1982. An SV40 deletion mutant accumulates late transcripts in a paranuclear extract. Virology **119:**1–11.
8. **Dildine, S. L.** 1992. Ph.D. dissertation. University of California, Irvine.
9. **Dildine, S. L., and B. L. Semler.** 1989. The deletion of 41 proximal nucleotides reverts a poliovirus mutant containing a temperature-sensitive lesion in the 5′ noncoding region of genomic RNA. J. Virol. **63:**847–862.

9a. **Dildine, S. L., and B. L. Semler.** 1992. Conservation of RNA-protein interactions among picornaviruses. J. Virol. **66:**4364–4376.

10. **Dildine, S. L., K. R. Stark, A. A. Haller, and B. L. Semler.** 1991. Poliovirus translation initiation: differential effects of directed and selected mutations in the 5′ noncoding region of viral RNAs. Virology **182:**742–752.

10a. **Dorner, A. J., B. L. Semler, R. J. Jackson, R. Hanecak, E. Duprey, and E. Wimmer.** 1984. In vitro translation of poliovirus RNA: utilization of internal initiation sites in reticulocyte lysate. J. Virol. **50:**507–514.

11. **Garcia-Blanco, M. A., S. F. Jamison, and P. A. Sharp.** 1989. Identification and purification of a 62,000-dalton protein that binds specifically to the polypyrimidine tract of introns. Genes Dev. **3:**1874–1886.
12. **Gebhard, J. R., and E. Ehrenfeld.** 1992. Specific interactions of HeLa cell proteins with proposed translation domains of the poliovirus 5′ noncoding region. J. Virol. **66:**3101–3109.
13. **Glass, J. M., X.-Y. Jia, and D. F. Summers.** 1993. Identification of the hepatitis A virus internal ribosome entry site: in vivo and in vitro analysis of bicistronic RNAs containing the HAV 5′ noncoding region. Virology **193:**842–852.
14. **Haller, A. A., and B. L. Semler.** 1992. Linker scanning mutagenesis of the internal ribosome entry site of poliovirus RNA. J. Virol. **66:**5075–5086.

14a. **Haller, A. A., and B. L. Semler.** Unpublished observations.

15. **Hamlyn, D. H., G. G. Brownlee, C. C. Cheng, M. J. Gait, and C. Milstein.** 1978. Complete sequence of constant 3′ noncoding regions on an immunoglobulin mRNA using the dideoxynucleotide method of RNA sequencing. Cell **15:**1067–1075.
16. **Helentjaris, T., E. Ehrenfeld, M. L. Brown-Luedi, and J. W. B. Hershey.** 1979. Alterations in initiation factor activity from poliovirus-infected HeLa cells. J. Biol. Chem. **254:**10973–10978.
17. **Hellen, C. U. T., G. W. Witherell, M. Schmid, S. H. Shin, T. V. Pestova, A. Gil, and E. Wimmer.** 1993. A cytoplasmic 57 kDa protein (p57) that is required for translation of picornavirus RNA by internal ribosome entry is identical to the nuclear polypyrimidine tract-binding protein. Proc. Natl. Acad. Sci. USA **90:**7642–7646.
18. **Jackson, R. J., M. T. Howell, and A. Kaminski.** 1990. The novel mechanism of initiation of picornavirus RNA translation. Trends Biochem. Sci. **15:**477–483.
19. **Jacobson, S. J., D. A. M. Konings, and P. Sarnow.** 1993. Biochemical and genetic evidence for a pseudoknot structure at the 3′ terminus of the poliovirus RNA genome and its role in viral RNA amplification. J. Virol. **67:**2961–2971.
20. **Jang, S. K., H.-G. Kräusslich, M. J. H. Nicklin, G. M. Duke, A. C. Palmenberg, and E. Wimmer.** 1988. A segment of the 5′ nontranslated region of encephalomyocarditis virus RNA directs internal entry of ribosomes during in vitro translation. J. Virol. **62:**2636–2643.
21. **Jang, S. K., T. V. Pestova, C. U. T. Hellen, G. W. Witherell, and E. Wimmer.** 1990. Cap-independent translation of picornavirus RNAs: structure and function of the internal ribosomal entry site. Enzyme **44:**292–309.
22. **Jang, S. K., and E. Wimmer.** 1990. Cap-independent translation of encephalomyocarditis virus RNA: structural elements of the internal ribosomal entry site and involvement of a cellular 57-kD RNA-binding protein. Genes Dev. **4:**1560–1572.
23. **Kaminski, A., T. Howell, and R. J. Jackson.** 1990. Initiation of encephalomyocarditis virus RNA translation: the authentic initiation site is not selected by a scanning mechanism. EMBO J. **9:**3753–3759.
24. **Kitamura, N., B. L. Semler, P. G. Rothberg, G. R. Larsen, C. J. Adler, A. J. Dorner, E. A. Emini, R. Hanecak, J. J. Lee, S. van der Werf, C. W. Anderson, and E. Wimmer.** 1981. Primary structure, gene organization, and polypeptide expression of poliovirus RNA. Nature (London) **291:**547–553.
25. **Kozak, M.** 1989. The scanning model for translation: an update. J. Cell Biol. **108:**229–241.
26. **Kühn, R., N. Luz, and E. Beck.** 1990. Functional analysis of the internal translation initiation site of foot-and-mouth disease virus. J. Virol. **64:**4625–4631.
27. **Laemmli, U. K.** 1970. Cleavage of structural proteins during the assembly of the head of bacteriophage T4. Nature (London) **227:**680–685.
28. **LaMonica, N., and V. R. Racaniello.** 1989. Differences in replication of attenuated and neurovirulent polioviruses in human neuroblastoma cell line SH-SY5Y. J. Virol. **63:**2357–2360.
29. **Lawson, M. A., B. Dasmahapatra, and B. L. Semler.** 1990. Species-specific substrate interactions of picornavirus 3C proteinase suballelic exchange mutants. J. Biol. Chem. **265:**15920–15931.
30. **Lloyd, R. E., M. Grubman, and E. Ehrenfeld.** 1988. Relationship of p220 cleavage during picornavirus infection to 2A protease sequences. J. Virol. **62:**2480–2488.
31. **Luz, N., and E. Beck.** 1990. A cellular 57 kDa protein binds to two regions of the internal initiation site of foot-and-mouth disease virus. FEBS Lett. **269:**311–314.
32. **Macejak, D. G., and P. Sarnow.** 1991. Internal initiation of translation mediated by the 5′ leader of a cellular mRNA. Nature (London) **353:**90–94.
33. **Meerovitch, K., R. Nicholson, and N. Sonenberg.** 1991. In vitro mutational analysis of *cis*-acting RNA translational elements within the poliovirus type 2 5′ untranslated region. J. Virol. **65:**5895–5901.
34. **Meerovitch, K., J. Pelletier, and N. Sonenberg.** 1989. A cellular protein that binds to the 5′-noncoding region of poliovirus RNA: implications for internal translation initiation. Genes Dev. **3:**1026–1034.
35. **Meerovitch, K., Y. U. Svitkin, H. S. Lee, F. Lejbkowicz, D. J. Kenan, E. K. L. Chan, V. I. Agol, J. D. Keene, and N. Sonenberg.** 1993. La autoantigen enhances and corrects aberrant translation of poliovirus RNA in reticulocyte lysate. J. Virol. **67:**3798–3807.
36. **Morris, D. R., T. Kakegawa, R. L. Kaspar, and M. W. White.** 1993. Polypyrimidine tracts and their binding proteins: regulatory sites

for posttranscriptional modulation of gene expression. Biochemistry **32:**2931–2937.

37. **Najita, L., and P. Sarnow.** 1990. Oxidation-reduction sensitive interaction of a cellular 50-kD protein with an RNA hairpin in the 5′ noncoding region of the poliovirus genome. Proc. Natl. Acad. Sci. USA **87:**5846–5850.
38. **Nicholson, R., J. Pelletier, S.-Y. Le, and N. Sonenberg.** 1991. Structural and functional analysis of the ribosome landing pad of poliovirus type 2: in vivo translational studies. J. Virol. **65:**5886–5894.
39. **Nomoto, A., B. Detjen, R. Pozzatti, and E. Wimmer.** 1977. The location of the polio genome protein in viral RNAs and its implication for RNA synthesis. Nature (London) **268:**208–213.
40. **Oh, S.-K., M. P. Scott, and P. Sarnow.** 1992. Homeotic gene *Antennapedia* mRNA contains 5′-noncoding sequences that confer translational initiation by internal ribosome binding. Genes Dev. **6:**1643–1653.
41. **Pelletier, J., and N. Sonenberg.** 1985. Insertion mutagenesis to increase secondary structure within the 5′ noncoding region of a eukaryotic mRNA reduces translational efficiency. Cell **40:**515–526.
42. **Pelletier, J., and N. Sonenberg.** 1988. Internal initiation of translation of eukaryotic mRNA directed by a sequence derived from poliovirus RNA. Nature (London) **334:**320–325.
43. **Percy, N., G. J. Belsham, J. K. Brangwyn, M. Sullivan, D. M. Stone, and J. W. Almond.** 1992. Intracellular modifications induced by poliovirus reduce the requirement for structural motifs in the 5′ noncoding region of the genome involved in internal initiation of protein synthesis. J. Virol. **66:**1695–1701.
44. **Pestova, T. V., C. U. T. Hellen, and E. Wimmer.** 1991. Translation of poliovirus RNA: role of an essential *cis*-acting oligopyrimidine element within the 5′ nontranslated region and involvement of a cellular 57-kilodalton protein. J. Virol. **65:**6194–6204.
45. **Pilipenko, E. V., V. M. Blinov, L. I. Romanova, A. N. Sinyakov, S. V. Maslova, and V. I. Agol.** 1989. Conserved structural domains in the 5′-untranslated region of picornaviral genomes: an analysis of the segment controlling translation and neurovirulence. Virology **168:**201–209.
46. **Pilipenko, E. V., A. P. Gmyl, S. V. Maslova, Y. V. Svitkin, A. N. Sinyakov, and V. I. Agol.** 1992. Prokaryotic-like cis-elements in the cap-independent internal initiation of translation on picornavirus RNA. Cell **68:**119–131.
47. **Racaniello, V. R., and D. Baltimore.** 1981. Molecular cloning of poliovirus cDNA and determination of the complete nucleotide sequence of the viral genome. Proc. Natl. Acad. Sci. USA **78:**4887–4891.
48. **Sanger, F., S. Nicklen, and A. R. Coulson.** 1977. DNA sequencing with chain-terminating inhibitors. Proc. Natl. Acad. Sci. USA **74:**5463–5467.
49. **Schwab, M., K. Alitalo, K.-H. Klempnauer, H. E. Varmus, J. M. Bishop, F. Gilbert, G. Brodeur, M. Goldstein, and J. Trent.** 1983. Amplified DNA with limited homology to *myc* cellular oncogene is shared by human neuroblastoma cell lines and a neuroblastoma tumour. Nature (London) **305:**245–248.
50. **Stein, O. E., and B. Moss.** 1990. Cytoplasmic expression system based on constitutive synthesis of bacteriophage T7 RNA polymerase in mammalian cells. Proc. Natl. Acad. Sci. USA **87:**6743–6747.
51. **Toyoda, H., M. Kohara, Y. Kataoka, T. Suganuma, T. Omata, N. Imura, and A. Nomoto.** 1984. Complete nucleotide sequences of all three poliovirus serotype genomes: implication for genetic relationship, gene function, and antigenic determinants. J. Mol. Biol. **174:**561–585.
52. **Trono, D., R. Andino, and D. Baltimore.** 1988. An RNA sequence of hundreds of nucleotides at the 5′ end of poliovirus RNA is involved in allowing viral protein synthesis. J. Virol. **62:**2291–2299.
53. **Vaheri, A., and J. S. Pagano.** 1965. Infectious poliovirus RNA: a sensitive method of assay. Virology **27:**435–436.
54. **Ypma-Wong, M. F., and B. L. Semler.** 1987. *In vitro* molecular genetics as a tool for determining the differential cleavage specificities of the poliovirus 3C proteinase. Nucleic Acids Res. **15:** 2069–2088.